



This is a repository copy of *Synthesis and Assembly of a Novel Glycan Layer in Myxococcus xanthus Spores*.

White Rose Research Online URL for this paper:
<http://eprints.whiterose.ac.uk/98268/>

Version: Accepted Version

Article:

Holkenbrink, C., Hoiczky, E., Kahnt, J. et al. (1 more author) (2014) Synthesis and Assembly of a Novel Glycan Layer in Myxococcus xanthus Spores. *Journal of Biological Chemistry*, 289 (46). pp. 32364-32378. ISSN 0021-9258

<https://doi.org/10.1074/jbc.M114.595504>

Reuse

Unless indicated otherwise, fulltext items are protected by copyright with all rights reserved. The copyright exception in section 29 of the Copyright, Designs and Patents Act 1988 allows the making of a single copy solely for the purpose of non-commercial research or private study within the limits of fair dealing. The publisher or other rights-holder may allow further reproduction and re-use of this version - refer to the White Rose Research Online record for this item. Where records identify the publisher as the copyright holder, users can verify any specific terms of use on the publisher's website.

Takedown

If you consider content in White Rose Research Online to be in breach of UK law, please notify us by emailing eprints@whiterose.ac.uk including the URL of the record and the reason for the withdrawal request.



eprints@whiterose.ac.uk
<https://eprints.whiterose.ac.uk/>

Synthesis and assembly of a novel glycan layer in *Myxococcus xanthus* spores*

Carina Holkenbrink^{1,4}, Egbert Hoiczky², Jörg Kahnt¹ and Penelope I. Higgs^{1,3}

¹Department of Ecophysiology, Max Planck Institute for Terrestrial Microbiology, 35043 Marburg, Germany

²The W. Harry Feinstone Department of Molecular Microbiology and Immunology, Johns Hopkins Bloomberg School of Public Health, Baltimore, MD 21205, USA

³Current address: Department of Biological Sciences, Wayne State University, 5047 Gullen Mall, Detroit, MI 48202

⁴Current address: Novo Nordisk Foundation Center for Biosustainability, University of Denmark, 2970 Hoersholm, Denmark

*Running title: *M. xanthus* spore wall synthesis and assembly

To whom correspondence should be addressed: Penelope I. Higgs, Department of Biological Sciences, Wayne State University, 5047 Gullen Mall, Detroit, MI, USA 48202, Tel.: (313) 577-9241; Fax: (313) 577-6891; E-mail: pihiggs@wayne.edu

Keywords: gram-negative bacteria; sporulation; polysaccharide; peptidoglycan; cell surface; membrane protein; *Myxococcus xanthus*

Background: During *Myxococcus xanthus* sporulation, a rigid coat is assembled on the cell surface.

Results: The coat consists of oligosaccharides (1 Glc : 17 GalNAc) and glycine which are absent or unprocessed in *exo* or *nfs* mutants.

Conclusion: The spore coat glycan is secreted by Exo- and rigidified by Nfs- machineries.

Significance: The spore coat is a novel *de novo* synthesized glycan layer.

ABSTRACT

Myxococcus xanthus is a Gram-negative deltaproteobacterium which has evolved the ability to differentiate into metabolically quiescent spores that are resistant to heat and desiccation. An essential feature of the differentiation processes is the assembly of a rigid, cell-wall-like spore coat on the surface of the outer membrane. In this study, we characterize the spore coat composition and describe the machinery necessary for secretion of spore coat material and its subsequent assembly into a stress-bearing

matrix. Chemical analyses of isolated spore coat material indicate that the spore coat consists primarily of short 1-4- and 1-3- linked GalNAc polymers which lack significant glycosidic-branching, and may be connected by glycine peptides. We show that 1-4 linked glucose (Glc) is likely a minor component of the spore coat with the majority of the Glc arising from contamination with extracellular polysaccharides (EPS), O-antigen, or storage compounds. Neither of these structures is required for the formation of resistant spores. Our analyses indicate the GalNAc/Glc polymer and glycine is exported by the ExoA-I system, a Wzy-like polysaccharide synthesis and export machinery. Arrangement of the capsular-like polysaccharides into a rigid spore coat requires the NfsA-H proteins, members of which reside in either the cytoplasmic membrane (NfsD, E, and G) or outer membrane (Nfs A, B, and C). The Nfs proteins function together to modulate the chain length of the surface polysaccharides, which is apparently necessary for their

assembly into a stress-bearing matrix.

Diverse bacterial genera have evolved to withstand unfavorable environmental conditions by differentiating into resting stages, termed spores or cysts (1). These entities are metabolically quiescent and display increased resistance to physical and chemical stresses. Spores, in particular, are resistant to high temperatures, sonic disruption, degradative enzymes, and periods of desiccation. Spore differentiation has been most intensively studied for endospores, such as those produced by the Gram-positive *Bacillus subtilis*. Endospores are produced within the protective environment of a mother cell which supplies many of the enzymes necessary to build the spore coat (2). An entirely different model system for spore differentiation is that of the Gram-negative *Myxococcus xanthus* in which the entire 0.5 x 7 μm rod-shaped vegetative cell rearranges into a spherical spore of approximately 1.7 μm in diameter without the protective environment of a mother cell.

A core feature of environmentally resistant spores is a dramatically altered cell envelope that contributes to the resistance features of spores. The composition and assembly of the spore cell envelope varies considerably between different spore formers, and many details of the respective assembly process have not yet been determined (3-6). In the case of *B. subtilis*, the spore coat is comprised of an altered and thickened peptidoglycan sacculus (termed the spore cortex) surrounded by a protein-rich coat (4); some spores additionally contain a mucous layer apparently comprised of soluble peptidoglycan fragments (7). In contrast, the *M. xanthus* spore coat material is primarily carbohydrate-rich and must be deposited on the outside of the outer membrane in a process that is directed from within the sporulating cell. Interestingly, in *M. xanthus*, the peptidoglycan layer appears to be degraded during spore differentiation and the spore coat layer likely replaces its function (5,8).

Our previous work identified two genetic loci, *exoA-H* and *nfsA-H*, important for production and assembly of the spore coat, respectively (5,9). Disruption of either (or both)

of these loci results in a phenotype in which cells initiate shape re-arrangement from rod to sphere, but subsequently revert to rod-shaped cells. Reversion is preceded by a transient stage of cell fragility and severe shape deformations (branching and formation of spiral cells) which are reminiscent of phenotypes observed in certain *E. coli* mutants defective in peptidoglycan synthesis (10). Electron microscopy analyses revealed that an *exoC* mutant lacks an obvious spore coat, while a Δ *nfsA-H* mutant produces a highly amorphous unstructured spore coat reminiscent of capsular material (5). Together, these observations suggest that assembly of a rigid, stress-bearing spore coat prior to removal of the periplasmic peptidoglycan is an essential step of spore differentiation.

The exact function of the Exo and Nfs machineries is not known. Some of the Exo proteins share homology with polysaccharide secretion machinery (5,11), and the Nfs proteins share homology with proteins (Glt) that may power the *M. xanthus* gliding motility machinery (12). It has been demonstrated that both the Glt and Nfs machinery appear to be involved in proton motive force-dependent possessive transport processes, but the consequence and details of this mechanism remain undiscovered (13).

In the present study, we set out to clarify the function of the Nfs and Exo protein machineries by characterizing the composition of the *M. xanthus* spore coat in *exo* and *nfs* mutants relative to the wild type. Composition and subunit linkage analysis of spore coat material isolated from the wild type suggest that the spore coat primarily consists of 1-4- and 1-3- linked GalNAc polymers with very little O-glycosidic branching. We confirmed that glycine is a major component of the spore coat material, but demonstrated that glucose, which is 1-4 linked, is only a minor component of the spore coat material; the majority of the detected glucose arises from contamination with storage compounds and EPS¹ and/or O-antigen. We show that ExoA-G, H and I are essential for export of at least the GalNAc and glycine components, and that NfsA-H form cell envelope

spanning machinery, which is necessary for appropriate processing of surface polysaccharides into short surface oligosaccharides necessary to form a rigid three-dimensional network.

EXPERIMENTAL PROCEDURES

Bacterial strains and growth conditions - Bacterial strains and plasmids are listed in Table 1. *M. xanthus* strains were cultivated at 32°C on CYE medium plates or in CYE broth (14,15). CYE agar was supplemented with 10 µg ml⁻¹ oxytetracycline or 100 µg ml⁻¹ kanamycin, where necessary. *E. coli* strains were grown at 37°C on LB medium plates or broth (16), supplemented with 50 µg ml⁻¹ kanamycin, 100 µg ml⁻¹ ampicillin or 100 µg ml⁻¹ spectinomycin, as appropriate.

Plasmid and strain construction - Primers used to generate plasmids are listed in Table S1. Template for PCR amplifications was genomic DNA isolated from *M. xanthus* strain DK1622, unless otherwise indicated. The insert regions for all plasmids generated was sequenced to confirm the absence of PCR generated errors. At least three independent *M. xanthus* clones for each mutant were tested to confirm stable and identical phenotypes.

Constructs used to generate markerless in-frame deletions in *M. xanthus* genes were constructed as previously described (15) in which DNA fragments of approximately 500 bp up- and downstream of the target gene were individually amplified and then fused. The resulting inserts were then cloned into pBJ114 (*galK*, kan^R) using the EcoRI / HindIII sites (plasmids pCH48 and pCH50), KpnI / HindIII sites (pCH62), or EcoRI / BamHI sites (all other plasmids). The resulting plasmids were introduced into *M. xanthus* DK1622 cells by electroporation, and homologous recombination into the chromosomes was selected by resistance to kanamycin. Deletions were selected by galactose-mediated counter selection (17) as described previously in detail (15).

Strains bearing interruptions in *wzm* or *epsV* were generated as follows: To be sure of an isogenic background, the DK1622 *wzm::Ωkan^R* mutant (PH1270) was recreated by transforming

DK1622 with genomic DNA isolated from strain HK1321 (18), followed by selection on CYE plates containing kanamycin. For disruption of *epsV*, a tetracycline resistant suicide vector was first generated. An oxytetracycline resistance cassette was PCR amplified from pSWU30 using primers oPH1315/oPH1316, and inserted into the BamHI and/ HindIII sites of pUC19. Next, an internal fragment of *epsV* (codons 323-500) was PCR amplified using primers oPH1313/oPH1314 and inserted into the EcoRI and BamHI sites, generating pCH19. To generate strain PH1285 (*wzm epsV*), pCH19 was introduced by electroporation into PH1270, and its integration into the *epsV* region *via* homologous recombination was selected by plating cells on CYE medium plates containing oxytetracycline and kanamycin. Strain PH1296 (*ΔexoC wzm epsV*) was obtained by transforming strain PH1261 (*ΔexoC*) with plasmid pCH19 and positive clones were selected by plating the transformants on CYE plates containing oxytetracycline followed by screening as above. The resulting strain was transformed with genomic DNA isolated from strain PH1270, and positive clones were selected on kanamycin. For all *epsV* strains, the successful integration of pCH19 in the genome was demonstrated by PCR amplification using primers oPH1352 and oPH1316, which bind in the region upstream of *epsV* and in the oxytetracycline resistance cassette, respectively.

Plasmids for production of Nfs proteins in *E. coli* were generated as follows: Plasmid pCH20 contained the *nfsA-C* region cloned into the NcoI and BamHI sites of the pCDF-Duet vector. To circumvent the intrinsic NcoI site in *nfsC* (near codon 327), the region was cloned in two steps. First, the 3' fragment of *nfsC* was amplified using primers oPH1376 / oPH1377 and cloned into the NcoI / BamHI sites of pCDF. Subsequently, a fragment containing *nfsA, B* and the 5' *nfsC* region was amplified using primers oPH1374 / oPH1375 and cloned into NcoI site, generating pCH20. Plasmid pCH21 contained the *nfsD-H* region in the NdeI / KpnI sites of the plasmid pCOLA-Duet. As PCR amplification of the entire 8.5 kb region was not successful, the coding region was cloned in two steps by taking

advantage of the native BbvCI site in the intergenic region between *nfsE* and *nfsF*. First, the *nfsD-E* region was amplified using primers oPH1378/oPH1392 and inserted into the NdeI / KpnI sites of the pCOLA-Duet. Next, the *nfsF-H* region was PCR amplified using primers oPH1393 / oPH1379 and inserted into the BbvCI / KpnI restriction sites, generating pCH21. To generate pCH57, the *nfsC* coding region was PCR amplified using primers oPH1478 / oPH1479 and inserted into the NdeI / KpnI sites of pCDF.

Induction of sporulation - Sporulation was chemically induced by addition of glycerol to *M. xanthus* vegetative broth cultures (3,19). Specifically, *M. xanthus* were inoculated into CYE broth and grown with aeration at 32° C to an optical density at 550 nm (OD₅₅₀) of 0.25 - 0.3. Sterile 10 M glycerol was added to 0.5 M final concentration and incubation continued as above for the indicated hours. To ensure good sporulation efficiency (~90%), a growth medium to flask ratio of 1:12.5 with a shaking speed of 220 rpm (for 250 ml flasks) and 105 rpm (for 5 L flasks) was used. To monitor sporulation, samples were withdrawn at various intervals after induction with glycerol and examined by DIC and/or light microscopy. Images were recorded with a Zeiss Axio Imager.M1 microscope (Carl Zeiss, Germany) equipped with a Cascade 1K camera (Visitron Systems, Germany).

To measure sporulation efficiency, cells were harvested by centrifugation (4618 x g for 10 min at 22°C) 24 hours after glycerol addition, resuspended in 500 µl H₂O, and dispersed with a FastPrep 24 cell homogenizer (MP Biomedicals, Solon, USA) for 20 s at 4.5 m/s. The spores were heated at 50°C for 1 h and then twice sonicated using a Branson sonifier 250 (15 bursts, output 3; duty cycle 30%) with intermediate cooling. Spores were enumerated using a Helber bacterial counting chamber (Hawksley, United Kingdom). Sporulation efficiency was calculated as the number of heat- and sonication-resistant spores normalized to the number of vegetative cells immediately prior to glycerol addition (determined from the OD₅₅₀, where OD 0.7 = 4 x 10⁸ cells ml⁻¹). Sporulation efficiency was

recorded as the average and associated standard deviation from three biological replicates and then normalized to the wild type (set at 100%).

Spore coat isolation - Spore coats were isolated from spores treated with glycerol for four hours using a protocol modified from (3). 800 ml of spore culture were harvested (4618 x g for 10 min at 22°C) and the pellets were frozen at -20°C until use. The pellet was resuspended in 8 ml of 50 mM Tris buffer pH 8.3, and 500 µl aliquots were added to 2 ml screw cap tubes containing 650 mg of 0.1 mm silica beads (Carl Roth, Germany). Spores were disrupted in a FastPrep 24 cell homogenizer (MP Biomedicals, Solon, USA) six times at 6.5 m s⁻¹ for 45 sec, with 2 min cooling on ice between shaking. Complete cell lysis was confirmed by microscopy. Lysates were pooled, the volume recorded, and the protein concentration was determined by Bradford assay (Bio-Rad, Hercules, USA) according to manufacturer's instructions. Spore coat material was pelleted at 40 000 x g for 30 min at 4°C (rotor MLA-55, Beckman Coulter, Brea, USA), washed twice with 7 ml 50 mM Tris buffer pH 8.3, resuspended in 3.3 ml 100 mM ammonium acetate (pH 7) containing 200 µg ml⁻¹ lysozyme, and incubated overnight (12-16 h) at 37°C with shaking at 200 rpm. Spore coats were again pelleted as above, washed once and resuspended in 7 ml 50 mM Tris buffer (pH 8.3). 375.7 µl 10% SDS and 35.7 µl 20 mg ml⁻¹ proteinase K were added and the solution was incubated for four hours at 37°C with shaking at 220 rpm. The spore coats were pelleted as above, resuspended in 1% SDS, pelleted, washed twice with 7 ml ddH₂O, and resuspended in 300 µl ddH₂O.

Electron microscopy - Samples were applied to glow-discharged carbon-coated 400 mesh copper grids and stained for one minute at room temperature using either unbuffered 2% uranyl acetate or 1% phospho tungsten at pH 7.5. Excess stain was removed with a filter paper and the grids were examined using a Philips CM12 microscope at an acceleration voltage of 80 kV. Images were recorded on Kodak ISO 165 black and white film at a nominal magnification of 52 000x.

Thin layer chromatography (TLC) - The isolated spore coat material was analyzed by TLC following modification of a protocol (20). The isolated spore coat material (~4.5 mg) was acid hydrolyzed by incubation in 3 M HCl at 105°C for three hours. To reduce the acidity, the samples were evaporated under vacuum until the volume was reduced to approximately 20 µl and then diluted in 500 µl water. This step was repeated. 2 µl samples corresponding to 0.2 mg protein of the original lysate and 2 µl of a standard solution containing 10 mM each galactosamine, glycine, glutamate and alanine were spotted onto a cellulose TLC plate and dried with a heat gun. The spots were resolved using a mobile phase consisting of n-butanol, pyridine and hydrogen chloride (2.5:1.5:1). The TLC plate was dried with a heat gun, stained (25 mg ninhydrin in 5:1 isopropanol:H₂O), and then dried with a heat gun until colored spots appeared. Each of the three spots identified from the wild type sample was analyzed further by mass spectrometry. Briefly, areas corresponding to the relative position of the spots were cut from the unstained TLC plate and soaked in 20 µl of 80% acetonitrile:0.04% TFA for 20 min at room temperature. 1 µl of the solvent was used for mass spectrometry analysis (4800Plus MALDI-TOF/TOF mass spectrometer, Applied Biosystems). An area of the TLC plate without sample material served as a negative control.

Glycosyl composition analysis - The glycosyl composition was determined by a combination of gas chromatography and mass spectrometry of acid hydrolysed per-*O*-trimethylsilyl derivatives of the monosaccharides performed by the Complex Carbohydrate Research Center (CCRC) in Atlanta, Georgia, USA. 200 to 400 µg of isolated spore coat material were supplemented with 20 µg inositol as an internal standard and lyophilized. Methyl glycosides were then prepared from the dry sample by methanolysis in 1 M HCl in methanol at 80°C (approx. 16 hours), followed by re-*N*-acetylation with pyridine and acetic anhydride in methanol (for detection of amino sugars). The sample was then per-*O*-trimethylsilylated by treatment with Tri-Sil (Pierce) at 80°C (0.5 hours). These procedures were carried out as

previously described in (21). GC/MS analysis of the TMS methyl glycosides was performed on an Agilent 6890N GC interfaced to a 5975B MSD, using a Supelco EC-1 fused silica capillary column (30m × 0.25 mm ID) (22). For each sample, the total mass, percent carbohydrate, and mass and corresponding molar percent of each carbohydrate detected were reported by CCRC. Total mass and mass of each component were subsequently normalized to 10⁸ cells as determined from optical density of the culture prior to induction of sporulation (Sup. Data File 1).

Glycosyl linkage analysis - For glycosyl linkage analysis, the spore coat polysaccharides were converted into methylated alditol acetates and analyzed by gas chromatography-mass spectrometry performed by the CCRC in Atlanta, Georgia, USA. 1.3 mg of isolated spore coat material was acetylated with pyridine and acetic anhydride and subsequently dried under nitrogen. The dried samples were suspended in 200 µl dimethyl sulfoxide and stirred for three days. The polysaccharides were permethylated by treatment with sodium hydroxide for 15 min followed by the addition of methyl iodide in dry dimethyl sulfoxide for 45 min (23). The procedure was repeated once to ensure complete methylation of the polysaccharide. The polymer was hydrolyzed by the addition of 2 M TFA for 2 hours at 121°C. The carbohydrates were then reduced with NaBD₄ and acetylated using a mixture of acetic anhydride and pyridine. The partially permethylated, depolymerized, reduced and acetylated monosaccharides were then separated by gas chromatography (30 m RTX 2330 bonded phase fused silica capillary column) and analyzed by mass spectrometry using an Agilent 6890N GC interfaced to a 5975B MSD (21). All detected linkages from each residue were recorded as percent present. Detected GalNAc or Glc linkages were summed and reported as percent of total GalNAc or Glc; the average of two independent analyses was reported. Raw data and calculations are reported in Sup. Data File 1.

Sucrose density gradient fractionation - Vectors pCH20, pCH21 and pCH57 (for production of NfsAB, NfsD-G, and NfsC,

respectively) were expressed in *E. coli* BL21 DE3. For Nfs protein expression, 1 L of LB medium supplemented with spectinomycin or kanamycin was inoculated 1:100 with an overnight culture of each strain, and grown at 37 °C with shaking. At OD 0.3, the cells were induced with 1 mM IPTG for 1 h. Cells were then harvested at 6000 x g for 20 min at 4°C. The cells were washed with 10 ml of 10 mM HEPES buffer (pH 7.8) at 4°C and the cell pellet was frozen at -20°C until use. Pellets were thawed on ice, resuspended in 10 ml 10 mM HEPES buffer (pH 7.8) containing 100 µl of mammalian protease inhibitor cocktail (Sigma Aldrich, St. Louis, USA), and lysed by French-press three times at approximately 20 000 psi. Unlysed cells were removed by centrifugation at 3500 x g for 10 min at 4°C. The cell lysate (2.2 ml) was loaded on a cold sucrose gradient consisting of 2.6 ml 55%, 4.8 ml 50%, 4.8 ml 45%, 4.8 ml 40%, 4.8 ml 35%, 4.8 ml 30%, 2.6 ml 25% sucrose as per (tubes 355631, Beckman, Brea, USA) (24,25). The gradient was centrifuged at 175 000 x g for ~16 hours at 4°C in a swinging bucket rotor (Rotor SW-32Ti, Beckman, Brea, USA). 1.7 ml fractions were harvested from the gradient top and stored at -20°C until use.

Proteins were precipitated from 1.6 ml of each fraction by addition of 216 µl of ice cold 100% TCA followed by incubation on ice for 5 min and then centrifugation at 16 200 x g for 5 min at 4°C. The protein pellets were washed with 2 ml of 100 mM Tris, pH 8 centrifuged as above for 5 min at 4°C, and resuspended in 100 µl 100 mM Tris pH 8. 100 µl 2 x LSB sample buffer (0.125 M Tris pH 6.8, 20% glycerol, 4% SDS, 10% β-mercaptoethanol) was added and samples were incubated at 99°C for 5 min. 5-20 µl of each these samples were analyzed on an 11% denaturing polyacrylamide gel (26) and the proteins were visualized by Coomassie stain [0.25% (w/v) ServaR, 50% ethanol, 7% acetic acid]. As controls, samples corresponding to an OD₅₅₀ of 0.1-0.2 of uninduced whole cells, induced whole cells, and induced cell lysate were also analyzed. To identify fractions enriched for the cytoplasmic membrane, the NADH oxidase activity was

determined in each fraction (24). NADH turnover was measured by addition of 25 µl of each gradient fraction to 500 µl of activity buffer (2.5 ml 1 M Tris adjusted with acetate to pH 7.9, 100 µl 100 mM DTT, 22.4 ml H₂O) plus 375 µl 0.1% NaHCO₃. The solution was thoroughly mixed and 100 µl of 0.2 mg ml⁻¹ NADH (in 0.1% NaHCO₃) was added. The solution was mixed by inversion and the absorbance at 340 nm was measured every six seconds for one minute in a quartz cuvette. The absorbance measurements were plotted and the slope (dA) of the graph was used to calculate the NADH oxidizing activity, where $U = 68 \times 10^{-1608} \times dA$.

Immunoblot analysis - Immunoblot analysis was performed as previously described using antisera at the following dilutions: anti-NfsA (1:400), anti-NfsB (1:1000), anti-NfsC and anti-NfsD (1:100), anti-NfsE (1:625) and anti-NfsG (1:500) (5). Anti-NfsC and -NfsE antisera were purified (27) prior to use.

RESULTS

EPS and/or O-Antigen co-purify with spore coat sacculi, but are not essential spore coat components - To understand how Exo and Nfs proteins function to secrete and assemble the spore coat, we set out to examine how strains bearing deletions in these machineries affected spore coat composition and structure. For these analyses, we started with the isolation and characterization of wild type spore coat material using adaptations of a previously described protocol (3) in which cells were chemically-induced to sporulate by treatment with 0.5 M glycerol for 4 hours. With this protocol, wild type spores yielded approximately 148 µg of isolated material per 10⁸ cells (Table 2). To examine the appearance of the isolated material, a portion of the sample was examined by negative stain electron microscopy. Similar to previous reports (3,8), wild type spore coats appeared as distinct spherical sacculi containing lesions, which were likely due to the mechanical disruption of the spores during coat isolation (Fig. 1, wt).

Previous analyses suggested that the wild type spore coat material contained high amounts of the carbohydrates N-acetyl-galactosamine

(GalNAc) and glucose (Glc) as well as the amino acids glycine (Gly) and alanine (Ala) (3,8). To confirm the carbohydrate composition of the wild type spore coat, ultimately in order to enable comparison to our mutant strains, we first examined the wild type material by acid hydrolysis followed by thin layer chromatography. Resolved samples were stained with ninhydrin to detect amino acids and amino sugars (Fig. 2). As controls, glutamate (Glu), Gly, Ala and GalN standards were separately analyzed (data not shown) or mixed and applied in a single lane (Fig. 2, lane 1). Three spots could be identified in wild type spore coat preparations: 1) a yellow stained spot ($R_f = 0.19$) corresponding to the GalN control, 2) a purple spot ($R_f = 0.06$) corresponding to the Gly control, and 3) an additional yellow spot ($R_f = 0.04$) which did not co-migrate with any of the standards (Fig. 2, lane 2). Each spot was scraped from the TLC plate and analyzed by mass spectrometry. Single compounds of 180.8 Da (spot 1) and 76.03 Da (spot 2) were detected; these corresponded exactly to the predicted masses of a protonated hexosamine and Gly, respectively. No compound could be detected for spot 3. Although previous analyses suggested Glc as a component of the spore coat (3), it was not detected by the ninhydrin stain as it does not contain reactive amino groups.

To assay the Glc content, and to obtain higher resolution and quantitative glycosyl composition of the spore coat material, the sample was additionally analyzed by combined gas chromatograph/mass spectrometry (GC/MS) of per-*O*-trimethylsilyl (TMS) derivatives of monosaccharides produced by acid hydrolysis (performed at the Complex Carbohydrate Research Center, Georgia, USA). These analyses indicated the isolated wild type spore coat consisted of approximately 92% carbohydrate material containing predominantly GalNAc [64 Mol percent (Mol%)], and Glc (20 Mol%) with lesser amounts of N-acetylglucosamine, rhamnose, xylose, mannose and galactose (Table 2 and Sup. Data File 1). It should be noted that because of the initial methanolysis and re-*N*-acetylation procedure, N-acetylation of all the spore coat glucosamine

pool is assumed; acetylation is consistent with previous labeling studies demonstrating incorporation of labeled acetate into the spore coat (28) (a modification which is lost during the acid hydrolysis step in the TLC analysis in Fig. 2).

Previous studies have demonstrated that almost all of the carbohydrate subunits identified in our analyses have been shown to be part of at least one of the two other cell surface polysaccharides of *M. xanthus*: the extracellular polymeric substances (EPS), and the O-antigen (O-Ag) component of the lipopolysaccharide (LPS) (29,30). To determine whether O-Ag or EPS play an essential role as a source of the spore coat components, or whether these components arise as a contamination due to co-purification, we generated a double mutant bearing disruptions in genes which have previously been shown to be necessary for O-antigen (*wzm*) (31) and EPS (*epsV*) synthesis (32). The *wzm epsV* double mutant formed as many heat and sonication-resistant spores as the wild type ($163 \pm 37\%$ vs. $100 \pm 20\%$, respectively) suggesting that neither of these products are essential for formation of resistant spores. Isolation of spore coat material from the *wzm epsV* mutant yielded approximately 89 μg per 10^8 cells corresponding to $\sim 60\%$ of the material isolated from the wild type (Table 2 and Sup. Data File 1). Examination of spore coat components by acid-hydrolysis and ninhydrin-stained TLC, revealed the same three spots identified in the wild type (Fig. 2, lane 4 vs. lane 2) suggesting a similar coat composition. However, quantitative glycosyl analysis indicated that the *wzm epsV* double mutant sample contained approximately 29%, 65%, and 58% of the wild type Glc, GalNAc and GlcNAc amounts and none of the rhamnose, xylose, mannose and galactose (Table 2 and Sup. Data File 1). Together, these results suggested that some of the Glc and GalNAc identified in the spore coat material, as well as all of the rhamnose, xylose, mannose and galactose likely come from contamination with O-Ag and/or EPS during the isolation procedure. The remaining GlcN(Ac) likely comes from peptidoglycan

remnants (given that ManNAc is unstable and degraded during the analysis).

The ExoC protein is necessary for export of GalNAc, Glc and Gly containing material - Our previous data indicated that ExoC, a predicted polysaccharide co-polymerase (Table 3 & Fig. 6), is necessary for secretion of spore coat material to the cell surface (5). To confirm these data and to identify specifically which components may be secreted by ExoC, we followed a similar protocol for spore coat isolation and characterization as described for the wild type above. Consistent with the lack of spore coat material observed in our previous study, only approximately 46 μg material per 10^8 cells (~31% of wild type material) could be isolated from the ΔexoC mutant (Table 2). Negative stain EM demonstrated that the ΔexoC sample consisted primarily of fibrous material associated with ring-like structures (Fig. 1, ΔexoC); importantly, no sacculi could be detected. When this material was subjected to analysis by ninhydrin-stained TLC, none of the three spots observed in the wild type sample could be detected (Fig. 2, lane 3), suggesting that *exoC* is necessary for incorporation of at least GalNAc and glycine into the spore coat.

To determine specifically which components were lacking in the ΔexoC mutant, we next subjected the material isolated from ΔexoC spores to quantitative glycosyl analysis. This material consisted of less carbohydrate (approx. two-thirds of the wild type percent carbohydrate) suggesting that ΔexoC reduced total carbohydrates isolated but did not necessarily affect other spore coat components. Consistent with the TLC analyses, no GalNAc could be detected (Table 2). Interestingly however, ~80% of the wild type Glc could still be detected. To further resolve whether ExoC is necessary for export of Glc or whether the remaining Glc arises from O-Ag and/or EPS, we generated a triple mutant bearing the *epsV* and *wzm* interruptions in the ΔexoC background. As expected, the chemical induced sporulation phenotype of this triple mutant phenocopied that of the single ΔexoC mutant; upon induction of sporulation, the cells rearranged to enlarged spheres which either failed to mature into phase

bright and resistant spores or reverted to rods (data not shown). The spore coat isolation protocol yielded approximately 8 μg material per 10^8 ΔexoC *epsV* *wzm* cells, corresponding to 9% and 18% of the material isolated from the *epsV* *wzm* and ΔexoC mutants, respectively (Table 2 and Sup. Data File 1). Negative stain EM demonstrated that in contrast to the fibrous like material observed in the isolated ΔexoC material (Fig. 1, ΔexoC), the ΔexoC *wzm* *epsV* material consisted entirely of kidney shaped globules (Fig. 1, ΔexoC *wzm* *epsV*). Quantitative glycosyl analysis indicated that this sample consisted of one-third less carbohydrate relative to the wild type of which 99.8% Mol% was Glc (Table 2 and Sup. Data File 1). The kidney-like shape and composition of this material are strikingly similar to glycogen granules previously characterized in other bacteria such as *Nostoc musorum* (33) suggesting that in the absence of all these export systems, the remaining isolated carbohydrate arises from glycogen which has previously been shown to accumulate prior to the onset of sporulation in *M. xanthus* (34). Furthermore, such granules could also be observed in the wild type EM analyses (arrows, Fig. 1 wt lower panel). Together these results suggest that the majority of the Glc observed in the spore coat material is due to contamination with EPS/O-Ag and cytoplasmic glycogen.

ExoB, C, D, E, G, H, and I are essential for spore coat synthesis - Our composition analysis suggested that at least ExoC is necessary to export spore coat polysaccharides containing GalNAc and Gly. However, *exoC* is encoded within an operon containing eight additional genes, *exoA-I* (5) (Table 3 & Fig. 6), and polysaccharide synthesis systems are often clustered and co-transcribed (35). To further define the system necessary to export spore coat material, we generated single in-frame deletion mutants of *exoB*, *exoD*, *exoE*, *exoF*, *exoG*, *exoH* and *exoI* and tested the mutants for production of resistant spores; *exoA* deletion mutants have previously been analyzed (36). For each of these strains, as well as the control ΔexoC , $\Delta\text{nfsA-H}$, and wild type strains, broth cultures were chemically induced to sporulate and the cell morphology was examined by differential

interference contrast (DIC) (T= 0, 4, 24 hours) and phase contrast (T= 4, 24 hours) microscopy (Fig. 3). The wild type rod-shaped cells (T=0) rearranged to spheres by 4 hours after induction and became phase bright between 4 and 24 hours after induction. In contrast, the $\Delta exoB$, D , E , G , H and I mutants phenocopied the $\Delta exoC$ and $\Delta nfsA-H$ mutants: cells formed enlarged spheres which failed to turn phase bright and sometimes reverted to misformed rod-shaped cells. $\Delta exoF$ mutants showed a partial phenotype in that some cells became misformed after induction, but the mutant produced similar numbers ($120 \pm 40\%$) of phase bright resistant spores as the wild type ($100 \pm 24\%$).

To examine whether these mutants were defective in spore coat production, spore coat material was isolated from each of the single mutants, acid hydrolyzed, and examined by ninhydrin-stained TLC. No spots corresponding to GalN(Ac) or glycine could be detected in $\Delta exoB$, C , D , E , G , H and I mutants, while $\Delta exoF$ mutants produced all spots with intensity similar to the wild type (Fig. 4). These results suggest that with the exception $exoF$, all other exo genes are essential for export of a polysaccharide containing at least GalNAc and Gly.

ExoA and ExoC/D belong to the Group C OPX and PCP-2a-like proteins, respectively, that form a terminal export complex for exopolysaccharides (Fig. 6), and these groups are predicted to be coupled to Wzy-dependent polymer biosynthesis pathways (11). In Wzy-dependent pathways, polyisoprenoid lipid undecaprenol diphosphate (und-PP) linked repeat units are generated at the inner leaflet of the cytoplasmic membrane, and then moved to the outer leaflet of the inner membrane by a flippase (Wzx) homolog (Fig. 6). No flippase homologs could be identified in the exo locus (Table 3), but two homologs (MXAN_1035 and MXAN_7416) were located elsewhere in the genome. To test whether either of these genes is necessary for spore production, we attempted to generate in-frame deletions of each and analyze the chemical-induced sporulation phenotype of the resultant strains. The $\Delta MXAN_1035$ mutant produced spherical cells that became phase

bright with the same timing and morphology as the wild type, but sporulation efficiency was reduced to $64 \pm 18\%$ of the wild type (Fig. 3). These results suggested that MXAN_1035 may function as a flippase with the Exo machinery, but that its function is partially redundant. We were unsuccessful in generating a deletion of MXAN_7416 and were therefore unable to examine whether this gene was involved in spore coat synthesis.

NfsA-H mutant cells produce intact spore coat sacculi composed of GalNAc, Glc and Gly - We next turned our attention to the role of the Nfs proteins (Fig. 6) in assembly of a compact spore coat. Our previous analyses indicated that the $\Delta nfsA-H$ mutant produced loosely associated and unstructured spore coat material on the surface of the cell, which could not function as a stress-bearing layer (5). To further define the function of the Nfs proteins, we set out to characterize how the nfs mutant spore coat material differed from that of the wild type using approaches outlined for the wild type and $exoC$ mutant. Using the spore coat isolation protocol, we obtained approximately 180 μg per 10^8 cells, corresponding to 121% of wild type material (Table 2 and Sup. Data File 1). Interestingly, negative stain electron microscopy analysis revealed that obvious spore coat sacculi could be identified although they appeared more unstructured than the wild type and tended to clump together (Fig. 1, Δnfs). These results suggested that the nfs mutant produced an intact spore coat sacculus, but that the composition or structure of the material is likely different from that of the wild type.

To address whether the composition of the $nfsA-H$ spore coat material differed from that of the wild type, we subjected the material to acid hydrolysis followed by ninhydrin-stained TLC. All three spots observed in the wild type sample (corresponding to GalN, Gly, and the unidentified component) could be detected in the $nfsA-H$ mutant (Fig. 2, lane 2 vs. lane 5). Quantitative glycosyl composition analyses suggested that the total amount of GalNAc and Glc was increased to 121 and 113%, respectively, of the wild type (Table 2 and Sup. Data File 1). An independent biological

replication of these analyses confirmed that the *nfs* mutant produced more total material and similarly increased relative levels of GalNAc and Glc over the wild type (data not shown). The molar ratio of GalNAc to Glc in the *nfs* mutant was 3.4 ± 0.1 compared to the wild type ratio of 2.8 ± 0.5 (data not shown). These data indicate that the spore coat of the *nfs* mutant does not lack a component of the spore coat, but that the Nfs complex is necessary for accumulation of appropriate levels of the spore coat material.

The nfs locus is necessary for polysaccharide chain length processing - Given that the *nfsA-H* mutant produced all the major spore coat components detected in the wild type, we next set out to determine whether the amorphous appearance of the spore coat could be a result of structural differences in polysaccharide arrangement. For this analysis, we first examined the linkages of the GalNAc and Glc residues in the spore coat material in the wild type and *nfs* mutant. Briefly, spore coat material was permethylated, acid hydrolyzed, and then acetylated such that free hydroxyl groups in the residue can be distinguished from those in glycosidic bonds by methylation vs. acetylation, respectively. The resulting monosaccharides were then analyzed by GC/MS to determine the relative derivate positioning.

Using this method, we first examined the wild type spore coat material and determined that GalNAc residues were 1-4-linked ($44 \pm 3\%$), 1-3-linked ($15 \pm 2\%$), or terminal (t) ($41 \pm 0\%$) (Table 4 and Sup. Data File 1). Glc residues were primarily identified as 1-4-linked ($64 \pm 3\%$) 1-6-linked ($6 \pm 3\%$) and terminal ($26 \pm 2\%$). None of the GalNAc and very little of the Glc ($\leq 2\%$) molecules had more than one linkage suggesting no detectable branching. Furthermore, relatively high proportions of terminal GalNAc and Glc residues were observed suggesting the chain length is relatively short. Interestingly, the Δ *nfsA-H* mutant spore coat material contained the same type of GalNAc and Glc linkages, but the proportion of internal residues was increased at the expense of terminal residues; GalNAc linkages detected were 1-4-linked ($63 \pm 8\%$), 1-3-linked ($32 \pm 5\%$), or terminal ($3 \pm 1\%$), and Glc linkages detected were 1-4-linked ($83 \pm 6\%$),

1-6-linked ($2 \pm 0\%$) or terminal ($12 \pm 3\%$) (Table 4 and Sup. Data File 1). Thus, the ratio of terminal to internal residues was decreased in the *nfs* mutants suggesting that the glycan chain length is longer than in the wild type. These data suggest that the Nfs proteins may be involved in chain length determination.

The Nfs proteins associate with the inner and outer membrane - We hypothesized that the Nfs proteins could mediate polysaccharide chain length either by affecting the synthesis of polysaccharides, which occurs at the cytoplasmic membrane, and/or by rearranging the polysaccharides after they have been secreted to the cell surface. To begin to distinguish between these possibilities, we set out to determine the exact compartment localization of the individual Nfs proteins. Since we have previously shown that NfsA, B, C, D, E and G, fractionate with the *M. xanthus* cell envelope (5), we now examined whether these proteins fractionate with the cytoplasmic or outer membranes.

We were unable to adapt other previously employed methods for separating *M. xanthus* OM and CM membranes, such as outer membrane isolation (40) or sucrose density gradient fraction (41) likely because the envelope characteristics of sporulating cells differs significantly from that of the vegetative cells for which they were developed. Therefore, we set out to examine the localization patterns of the Nfs proteins produced heterologously in *E. coli* with the well-defined and rigorous sucrose density gradient fractionation protocol (24,42). For this approach, the *nfs* operon was separated in two fragments (*nfsA-C* and *nfsD-H*) and cloned behind the IPTG-dependent T7-promotor of the pCDF (generating pCH20) and pCOLA (generating pCH21) plasmids, respectively. Each plasmid was induced with IPTG alone or together in *E. coli* BL21(DE3). Optimal production of NfsA, B, D, E, and G could be detected when pCH20 and pCH21 were expressed independently, but NfsC, NfsF, and NfsH could not be detected (data not shown). Optimal production of NfsC could be detected if *nfsC* was cloned alone into pCDF (generating pCH57) and expressed alone (data not shown).

NfsF and NfsH could not be detected likely because of the quality of the anti-sera (5).

To examine the localization patterns of the NfsA and B proteins, cell lysates from IPTG-induced *E. coli* BL21 expressing pCH20 were applied to a 25-55% sucrose step gradient, and centrifuged to allow CMs and OM to separate. To determine the relative position of OMs, each fraction was resolved by SDS-PAGE, stained by Coomassie Blue, and examined for the characteristic pattern of the *E. coli* OmpF/C proteins (Fig. 5A, lanes 15-18). To identify CM proteins, each fraction was assayed for peak NADH oxidase activity (Fig. 5A lanes 7-11). To identify the localization of NfsA and B, each fraction, as well as uninduced and induced whole lysates, was subjected to immunoblot analysis with anti-NfsA and anti-NfsB sera (Fig. 5A). NfsA (32 kDa) and NfsB (47 kDa) were identified in induced, but not uninduced, whole cells, and in fractions 14-18 consistent with OM localization (Fig. 5A). To examine the localization pattern of NfsC, cell lysates from *E. coli* BL21(DE3) expressing pCH57 were analyzed as described above, resulting in detection of NfsC in the induced, but not uninduced whole cell fractions and in fractions 14-18, concurrent with the OmpC/F OM marker proteins (Fig. 5B). Finally, to examine the localization patterns of NfsD, E, and G, cell lysates from *E. coli* BL21(DE3) expressing pCH21 were analyzed as described above, resulting in detection of NfsD, NfsE, and NfsG in the induced, but not uninduced, whole cell lysates and in fractions 7-12, consistent with the CM marker peak NADH oxidase activity. NfsG was detected at two co-fractionating bands suggesting the protein was partially degrading after cell lysis. These analyses strongly suggest that NfsA, consistent with its predicted β -barrel porin-like structure, NfsB, and NfsC, are OM-associated proteins, while NfsD, NfsE, and NfsG are CM-associated proteins (Fig. 6).

DISCUSSION

The goal of this study was to characterize the production of the *M. xanthus* spore coat - a remarkable cell wall-like structure

which surrounds the outer membrane of sporulating *M. xanthus* cells and which provides structural stability to the spore (5)(13). To begin to characterize this process, our approach was to take advantage of mutants in the *exo* and *nfs* operons, which we have previously shown encode proteins necessary for secretion and assembly of the spore coat, respectively (5). Thus, we performed a comparative analysis of spore coat material in these mutants versus the wild type.

Structure of the spore coat- Early composition analysis of the spore coat determined it consists primarily of carbohydrates (79%) with lesser amounts of protein (14%), but relatively high amounts of glycine (7%) (3). Specifically, it was proposed that the carbohydrate material consisted of GalNAc and Glc in a molar ratio of 3:1, and that Glc may form an independent polymer. Our current analyses refine these early observations. Quantitative GC/MS analysis of acid hydrolyzed purified material, confirmed that GalN (likely acetylated) and Glc are the primary carbohydrate components and can be detected in a molar ratio of 3.2:1 (Sup. Data File 1). However, our further analyses suggest that the actual GalNAc:Glc ratio is much higher because the majority of the Glc (~71%) arises from contamination with co-purifying EPS, O-Ag, or cytoplasmic storage compounds, such as glycogen (34). Although we had previously considered that the two surface polysaccharides may serve as essential components of the spore coat (either as attachment sites or saccharide sources), our observation that a mutant unable to produce EPS or O-Ag (*wzm epsV*) can produce resistant spores with equal efficiency as the wild type suggests they are merely contaminating substances. Consistently, the small amount of material which can be purified from the spore-coat deficient *exoC* mutant (5) consists of fibers that are reminiscent of isolated EPS (fibrils) (29) (Fig. 1). Furthermore, the material isolated from a triple mutant defective in spore coat and EPS/O-Ag (*exoC wzm epsV*) (Table 2) contained only glycogen-like particles (33) (Fig. 1) composed almost entirely (>99 Mol%) of glucose (Sup. Data File 1). We could detect similar particles in

the wild type spore coat preparations (Fig. 1, wt, indicated by arrows), and we suggest that the copurifying EPS-like fibers may have been trapped inside the wild type spore coat sacculi. Together, then, our results suggest that of the $\sim 24 \mu\text{g}$ of Glc isolated from 10^8 wild type cells, $\sim 17 \mu\text{g}$ ($\sim 70\%$) arises from EPS/O-Ag ($\mu\text{g Glc}_{\text{wt}} - \mu\text{g Glc}_{\text{wzm epsV}}$), $\sim 4 \mu\text{g}$ ($\sim 18\%$) arises from the spore coat ($\mu\text{g Glc}_{\text{wt}}$ minus $\mu\text{g Glc}_{\text{exoC}}$), and $\sim 2 \mu\text{g}$ ($\sim 10\%$) arises from storage compounds ($\mu\text{g Glc}_{\text{exoC wzm epsV}}$). Given that no GalNAc can be detected in the *exoC* mutant, we assumed that all of the isolated GalNAc arises from the spore coat material specifically. Inconsistent with this assumption, however, is the $\sim 35\%$ reduction of GalNAc observed in the *wzm epsV* mutant compared to the wild type ($61 \mu\text{g}$ vs. $94 \mu\text{g}$ GalNAc per 10^8 cells, respectively), which could suggest that some of the GalNAc arises from EPS and/or O-Ag. One possible interpretation of this discrepancy is that ExoC contributes to GalNAc incorporation into EPS and/or O-Ag synthesis. If this is the case, the interpretation is that the spore coat material contains $61 \mu\text{g}$ of GalNAc per 10^8 cells, with the molecular ratio of GalNAc:Glc at 11:1 (Sup. Data File 1). Alternatively, the reduction of GalNAc observed in the *wzm epsV* mutant may simply be an artifact arising from competition for the undecaprenyl diphosphate pool, which, in the *exoC* mutant, may be sequestered as spore coat precursors. In this case, we could assume the wild type spore coat contains $94 \mu\text{g}$ of GalNAc per 10^8 cells, and the molecular ratio of GalNAc:Glc is closer to 17:1; this is the interpretation we favor.

Consistent with early composition analysis (3), we could demonstrate that glycine (Gly) is readily detected in the spore coat material if the sample is analyzed by TLC. Interestingly, however, Gly could not be detected in the GC/MS analysis (Table 2 and data not shown). In the procedure used for GC/MS analysis, the lyophilized spore coat is first subject to acid-methanolysis, re-N-acetylated, and then per-O-trimethylated to volatilize components for gas chromatography. One possibility is that the Gly is lost early in the hydrolysis procedure. This could occur if the Gly

was attached via an amide bond to at least a portion of the GalN (in replacement of the acetyl-group; Fig. 6 inset). Such a configuration has been proposed for the heteropolysaccharide in the sheath of *Leptothrix cholodnii* (43). We hypothesize that in the GC/MS procedure, the initial hydrolysis step would remove the Gly (or acetyl group), and subsequently, due to the re-acetylation step, be detected only as GalNAc. In the TLC protocol, Gly or Ac groups removed during the acid hydrolysis step remain in the reaction mixture such that Gly is detected by ninhydrin stain. This hypothesis is consistent with the observations that 1) Gly is intimately connected with the polysaccharide synthesis and secretion because no Gly could be detected in the *exoC* mutant (this study), and 2) Gly incorporation into spore coat material is sensitive to bacitracin, which suggests it requires a lipid-pyrophosphate carrier (28).

To begin to understand how the spore coat components could be arranged to form a cell wall-like matrix, we performed linkage analysis on the glycosyl components of the spore coat and then focused on the GalNAc and Glc units. Linkage analysis revealed that the wild type isolated spore coat material contained GalNAc in t- (terminal), 1-4-, or 1-3- linkages in a ratio of 1:1:0.4 (Sup. Data File 1). Glc residues were detected primarily as t-Glc, and 1-4-Glc, in a ratio of 1:2.4 (Sup. Data File 1). The high proportion of terminal to internal residues, together with no detected O-glycosidic branching, suggests the glycans are surprisingly short. With this data alone, we were unable to ascertain exactly how long the chains may be because it is unknown which proportions of these linkages are due to contaminating Glc and GalNAc from the EPS/O-Ag and glycogen, and because it is unknown whether the Glc and GalNAc are both present in a single polymer. It has been previously proposed that the GalNAc and Glc form independent polymers based on the observation that later during sporulation, the Glc content continued to accumulate while GalNAc remained constant (3). In the light of our observation that the majority of the Glc arises from contamination with non-spore coat polysaccharides, we suggest that this may have

been due to the continued accumulation of glycogen.

Because the spore coat material is insoluble and highly resistant to enzymatic digestion (3), we did not ascertain its three-dimensional structure. Furthermore, initial attempts to isolate the lipid carrier linked polysaccharide subunit, which is likely used to synthesize the polysaccharide (see discussion on Exo below), were so far unsuccessful. Nevertheless, we propose that the conspicuous absence of significant dual linked Glc or GalNAc residues suggests no branching and implies that the individual polymers are not connected via O-glycosidic bonds. To form a rigid sacculus, the spore coat glycans are likely tightly associated. How could this be mediated? In plant or fungal cell walls, the respective Glc (cellulose) or GlcNAc (chitin) polymers are held together by hydrogen bonds from the hydroxyl or amine groups (44,45). In contrast, in peptidoglycan, glycan strands are connected via peptide bridges (46). Because a high proportion of Gly is present in the spore coat, we favor a structure in which the adjacent glycans chains are connected by Gly peptides. While in peptidoglycan the peptide bridges are connected to the 3 carbon of ManNAc via a lactyl ether bridge, we propose (as described above) that in the spore coat, a single glycine or a glycine peptide could form an N-glycosidic bond with the C1 atom of one polymer and a peptide bond with the nitrogen atom of a second polymer (Fig 6, inset). However, it is also possible that Gly peptides are linked via the C1-end of the polymer. These possible linkages have been proposed previously in the N-glycyl-glucosamine cell wall of *Halococcus morrhuae* (47), the poly-glutamine chain C1-terminally- linking two cell wall polymers in the archaeon *Natronococcus occultus* (48), or the heteropolysaccharide in the sheath of *Leptothrix cholodnii* (43). We cannot, however, rule out that Gly is incorporated directly in the polymer and that adjacent strands are held together by hydrogen bonds.

Given that the *nfs* mutant did not lack any of the identified spore coat components, we also rationalized that the misassembled spore coat observed in this mutant might be due to

perturbed glycan structure, and that comparative analysis between the wild type and *nfs* mutant would be an important tool to examine how the spore coat is structured and assembled. The most interesting observation from linkage analysis of the *nfs* spore coat material is the dramatic 39% reduction of terminal GalNAc residues and concurrent 18% increase each in ,4- and ,3-GalNAc residues (Sup. Data File 1). The remaining 3% loss of t-GalNAc appears to correlate with a small amount of ,3,4- and 4,6-linked GalNAc residues which were not observed in the wild type material. The reduction in terminal residues observed in the *nfs* mutant, together with extremely few tri-linked residues, strongly suggests that the chain length of the glycans in the spore coat is dramatically increased in the *nfs* mutant. Interestingly, the *nfs* mutation also affected the Glc linkages with 14%, 4%, reduction in t-Glc, and 1-6 linked Glc, residues, respectively, corresponding to a 19% increase in 1-4 linkages. The percent of Glc residues rearranged in the *nfs* mutant (19%), is similar to the proportion of Glc (18%) that we calculated as belonging to the spore coat itself (Sup. Data File 1). We took advantage of this observation to calculate the fraction of Glc linkages which differed between the wild type and *nfs* mutant coats, and then used this data to estimate the average chain length of the spore coat glycan. Given a terminal to internal ratio of altered Glc residues was 1:1.6, and the equivalent GalNAc ratio of 17:24.3, the average chain length of the glycans in the wild type would be 2.4 (Sup. Data File 1). Assuming an equivalent proportion of Glc are incorporated in the *nfs* mutant spore coat, the terminal to internal ratios for Glc and GalNAc would be 1:4 and 18:664, respectively. These data suggest the average chain length in the *nfs* mutant is 36, 15 times longer than in the wild type. These data suggest a short chain length is necessary for appropriate packing of the chains. Although we observed qualitatively similar amounts of Gly in the wild type and *nfs* mutant, it is not known if the Gly is correctly incorporated or linked, which may also contribute to the loss of the rigid sacculus.

Model for synthesis and assembly of the spore coat - Our analysis of the *exo* locus and

Nfs proteins allows us to propose a model for how the spore coat may be synthesized and assembled (Fig. 6). Bioinformatic, biochemical, and genetic analyses strongly suggest that spore coat polysaccharides containing 1-3- and 1-4-linked GalNAc, 1-4-linked Glc (GalNAc:Glc ~17:1) and Gly are secreted to the sporulating cell surface by the Exo proteins which function as a Wzy-dependent polysaccharide export pathway (11,35). Specifically, we propose that ExoE, an initiating sugar transferase homolog, likely links UDP-GalNAc (or UDP-Glc) to a polyisoprenoid lipid undecaprenol diphosphate (und-PP) lipid carrier (Fig. 6, step 1). ExoG, H, and I, which are predicted to be cytoplasmic proteins homologous to proteins that generate or modify nucleotide-activated sugars in pathways leading to polysaccharide synthesis (49), are likely necessary for generating precursors for ExoE, and/or for modifying the und-PP linked sugar repeat units. The complete absence of spore coat in *exoE*, *exoG*, *exoI*, and *exoH* mutants is consistent with a defect in precursor synthesis.

The lipid-linked sugar repeat unit is predicted to be transferred to the outer leaflet of the inner membrane by a flippase (Wzx) homolog (35) (Fig. 6, step 2). Two flippase homologs can be identified in the *M. xanthus* genome: MXAN_1035 and MXAN_7416, which are located in the vicinity of polysaccharide synthesis protein homologs previously implicated in EPS production (32,50). Based on the observation that deletion of MXAN_1035 had only a minor effect on sporulation, the most likely candidate is MXAN_7416. However, we were unable to delete this gene and attempts to demonstrate interactions between the MXAN_7416 and ExoC or the putative polymerase (MXAN_3026) proteins were not yet successful (data not shown). In the periplasm, the repeat units are linked to higher molecular weight polysaccharides by a polymerase (Wzy) homolog (51), which is most likely encoded by MXAN_3026 (5) (Fig.6, step 3).

The polymerized repeat units are then transported to the surface of the sporulating cell by a terminal transport complex consisting of at least ExoC, ExoD, and ExoA (Fig. 6). ExoA (a

homolog of Wza) likely forms homomultimers in the outer membrane forming a channel through which polysaccharides are extruded (11). ExoC and D form a split version of the copolymerase, Wzc, which contains an amino terminal copolymerase domain localized in the cytoplasmic membrane (ExoC) fused to a cytoplasmic tyrosine kinase domain (ExoD). It has been shown that the tyrosine autophosphorylation and dephosphorylation (mediated by a dedicated phosphatase, Wzb) cycles can regulate the amount of surface polysaccharide (52), and/or the chain length of the surface polysaccharides (53) perhaps by direct contact of the N-terminal Wzc domain with the Wza oligomer. ExoA, ExoC, and ExoD are all essential for formation of resistant spores and for spore coat production [(36,54,55) and this study], and it has been demonstrated that ExoD autophosphorylates and transfers a phosphoryl group to ExoC *in vitro* (55) (Fig 6, step 4). The function of the two remaining Exo proteins (B and F) is less clear. Our studies demonstrated that ExoB, a predicted outer membrane protein, is essential for sporulation and spore coat production, but it is not clear what specific role this protein plays in polysaccharide synthesis and secretion. Finally, our results suggest that ExoF, which is predicted to reside in the cytoplasm, is partially dispensable for spore coat production because the mutant accumulated spore coat material and displayed only a minor sporulation defect. ExoF is homologous to YvcK-like proteins. The exact function of YvcK is not known, but in *B. subtilis* YvcK is important for gluconeogenic growth (57) and ExoF might play a subtle role in metabolic rearrangements necessary for spore coat precursor generation by gluconeogenesis in *M. xanthus* (9).

Once secreted to the cell surface, the Nfs machinery is necessary for assembly of the glycans into a rigid compact cell wall-like layer capable of replacing the function of the degraded peptidoglycan (5,9). Our data suggest this process involves significantly decreasing the average chain length of the polysaccharides from an estimated 36 residues to 2.4. The eight Nfs proteins (A-H) form a functional complex because, with the possible exception of *nfsC*

which was not examined, all other *nfs* genes are necessary for mature spore formation, and the protein stability of most of the Nfs proteins is dependent upon the presence of the others (5). Using heterologous Nfs protein production, we showed here that the Nfs machinery spans the cell envelope with both outer membrane (NfsA, B, C) and inner membrane (NfsD, E, and G) associated proteins (Fig. 6). Specifically, we predict that NfsA (as well as NfsH which was not analyzed here), are integral porin-like proteins because they both contain predicted beta-barrel structures (5). NfsC, and NfsB are likely OM-associated proteins, and reiterative BLAST analysis of NfsB further suggests cell surface localization. NfsD contains a convincing transmembrane segment near the amino-terminus with the majority of the protein exposed to the periplasm. NfsG likely contains an internal transmembrane segment (aa ~376-390) (58) with a cytoplasmic exposed N-terminal region and a periplasmic exposed C-terminal region. NfsE is a predicted lipoprotein and in our heterologous system it was located in the CM. This finding should be interpreted with caution since NfsE does not contain the *E. coli* CM localization signal (Asp at position +2), or the recently suggested *M. xanthus* CM localization signal (K at +2) (59). However, the NfsE homolog, GltE, has been previously shown to fractionate with the CM (12), although it was later depicted in the OM (13). The localization of NfsF is not clear because it cannot be detected with our antisera; however, the protein is predicted to be located in the periplasm.

What specifically does the Nfs complex do? Our analyses suggested that the Nfs complex is not only necessary for appropriate chain length of the secreted glycans, but also for the appropriate total quantity because the per cell spore coat material isolated from *nfs* mutants was more abundant (this study and (5)). It was recently demonstrated that at least NfsG rotates around the pre-spore periphery in a process likely mediated by NfsG-dependent coupling to the AglQRS (Exb/Tol/Mot family) complex

thought to harness proton motive force (pmf) (13). Because analysis of these proteins with respect to sequence homology reveals little as to their molecular function, how they exert the observed effects on spore coat poly/oligosaccharide chain length remains speculative: One possibility is that the Nfs complex is necessary for cleavage of the surface polysaccharides (Fig. 6, step 5a) in order to subsequently mediate crosslinks between glycans. Perhaps, the rotating complex is necessary to provide directionality and order to this process. Although pmf is clearly required for this process, the movement may be a consequence of its enzymatic processivity like peptidoglycan synthesis drives the movements of MreB-associated peptidoglycan synthase complexes (60,61).

Given that control of polysaccharide chain length and surface abundance has previously been attributed to tyrosine phosphorylation cycles in Wzc homologs (52,53), an alternate possibility is that the Nfs complex could affect the chain length of surface poly/oligosaccharides by modulating the activity of ExoC/D (Fig. 6 step 5b). Interestingly, a phosphopeptide binding FHA (Forkhead associated) domain (62) is predicted in the amino terminal domain of NfsG which could provide a mechanism for direct interaction between NfsG and phosphorylated ExoC/D [and/or a putative Wzb (phosphatase) homolog which are thought to be involved in phospho-tyrosine regulation of Wzc proteins (11)]. It may be that shorter fragments are necessary to generate a structurally rigid matrix because they facilitate appropriate packing on the prespore surface. Perhaps the rotating Nfs complex functions as a timed regulator to generate an appropriate mix of short and long fragments by “resetting” the individual Exo complexes as it passes. Ongoing efforts to solve the three dimensional structure of this fascinating biological structure will surely provide deeper insights as to the mechanism of action of the Nfs machinery as well as that of Exo.

REFERENCES

1. Shimkets, L., and Brun, Y. V. (2000) Prokaryotic Development: Strategies to enhance survival. in *Prokaryotic Development* (Shimkets, L., and Brun, Y. V. eds.), American Society for Microbiology. pp 1-7
2. Higgins, D., and Dworkin, J. (2012) Recent progress in *Bacillus subtilis* sporulation. *FEMS Microbiol Rev* **36**, 131-148
3. Kottel, R. H., Bacon, K., Clutter, D., and White, D. (1975) Coats from *Myxococcus xanthus*: characterization and synthesis during myxospore differentiation. *J Bacteriol* **124**, 550-557
4. McKenney, P. T., Driks, A., and Eichenberger, P. (2013) The *Bacillus subtilis* endospore: assembly and functions of the multilayered coat. *Nat Rev Microbiol* **11**, 33-44
5. Müller, F. D., Schink, C. W., Hoiczky, E., Cserti, E., and Higgs, P. I. (2012) Spore formation in *Myxococcus xanthus* is tied to cytoskeleton functions and polysaccharide spore coat deposition. *Mol Microbiol* **83**, 486-505
6. Flardh, K., and Buttner, M. J. (2009) *Streptomyces* morphogenetics: dissecting differentiation in a filamentous bacterium. *Nat Rev Microbiol* **7**, 36-49
7. Faille, C., Ronse, A., Dewailly, E., Slomianny, C., Maes, E., Krzewinski, F., and Guerardel, Y. (2014) Presence and function of a thick mucous layer rich in polysaccharides around *Bacillus subtilis* spores. *Biofouling* **30**, 845-858
8. Bui, N. K., Gray, J., Schwarz, H., Schumann, P., Blanot, D., and Vollmer, W. (2009) The peptidoglycan sacculus of *Myxococcus xanthus* has unusual structural features and is degraded during glycerol-induced myxospore development. *J Bacteriol* **191**, 494-505
9. Müller, F. D., Treuner-Lange, A., Heider, J., Huntley, S. M., and Higgs, P. I. (2010) Global transcriptome analysis of spore formation in *Myxococcus xanthus* reveals a locus necessary for cell differentiation. *BMC genomics* **11**, 264
10. Nelson, D. E., and Young, K. D. (2001) Contributions of PBP 5 and DD-carboxypeptidase penicillin binding proteins to maintenance of cell shape in *Escherichia coli*. *J Bacteriol* **183**, 3055-3064
11. Cuthbertson, L., Mainprize, I. L., Naismith, J. H., and Whitfield, C. (2009) Pivotal roles of the outer membrane polysaccharide export and polysaccharide copolymerase protein families in export of extracellular polysaccharides in gram-negative bacteria. *Microbiol Mol Biol Rev* **73**, 155-177
12. Luciano, J., Agrebi, R., Le Gall, A. V., Wartel, M., Fiegna, F., Ducret, A., Brochier-Armanet, C., and Mignot, T. (2011) Emergence and modular evolution of a novel motility machinery in bacteria. *PLoS Genet* **7**, e1002268
13. Wartel, M., Ducret, A., Thutupalli, S., Czerwinski, F., Le Gall, A. V., Mauriello, E. M., Bergam, P., Brun, Y. V., Shaevitz, J., and Mignot, T. (2013) A versatile class of cell surface directional motors gives rise to gliding motility and sporulation in *Myxococcus xanthus*. *PLoS Biol* **11**, e1001728
14. Campos, J. M., and Zusman, D. R. (1975) Regulation of development in *Myxococcus xanthus*: effect of 3':5'-cyclic AMP, ADP, and nutrition. *Proc Natl Acad Sci U S A* **72**, 518-522
15. Lee, B., Schramm, A., Jagadeesan, S., and Higgs, P. I. (2010) Two-component systems and regulation of developmental progression in *Myxococcus xanthus*. *Methods Enzymol* **471**, 253-278
16. Maniatis, T., Fritsch, E. F., and Sambrook, J. (1982) *Molecular cloning, A Laboratory Manual.*, Cold Spring Harbor Laboratory Press, Cold Spring Harbor, NY
17. Ueki, T., Inouye, S., and Inouye, M. (1996) Positive-negative KG cassettes for construction of multi-gene deletions using a single drug marker. *Gene* **183**, 153-157
18. Guo, D., Bowden, M. G., Pershad, R., and Kaplan, H. B. (1996) The *Myxococcus xanthus* rfbABC operon encodes an ATP-binding cassette transporter homolog required for O-antigen biosynthesis and multicellular development. *J Bacteriol* **178**, 1631-1639
19. Dworkin, M., and Gibson, S. M. (1964) A system for studying microbial morphogenesis: rapid formation of microcysts in *Myxococcus xanthus*. *Science* **146**, 243-244
20. Chaplin, M. C. (1986) Monosaccharides. in *Carbohydrate analysis- a practical approach* (Chaplin, M. C., and Kennedy, J. F. eds.), IRL Press, Oxford. pp 1-36
21. York, W. S., Darvill, A. G., McNeil, M., and Stevenson, T. T. (1985) Isolation and characterization of plant cell walls and cell wall components. *Methods Enzymol* **118**, 3-40

22. Merkle, R. K., and Poppe, I. (1994) Carbohydrate composition analysis of glycoconjugates by gas-liquid chromatography/mass spectrometry. *Methods Enzymol* **230**, 1-15
23. Ciucanu, I., and Kerek, F. (1984) A simple and rapid method for the permethylation of carbohydrates. *Carbohydr Res* **131**, 209-217
24. Osborn, M. J., Gander, J. E., and Parisi, E. (1972) Mechanism of assembly of the outer membrane of *Salmonella typhimurium*. Site of synthesis of lipopolysaccharide. *J Biol Chem* **247**, 3973-3986
25. Letain, T. E., and Postle, K. (1997) TonB protein appears to transduce energy by shuttling between the cytoplasmic membrane and the outer membrane in *Escherichia coli*. *Mol Microbiol* **24**, 271-283
26. Laemmli, U. K. (1970) Cleavage of structural proteins during the assembly of the head of bacteriophage T4. *Nature* **227**, 680-685
27. Koelle, M. R., and Horvitz, H. R. (1996) EGL-10 regulates G protein signaling in the *C. elegans* nervous system and shares a conserved domain with many mammalian proteins. *Cell* **84**, 115-125
28. Filer, D., White, D., Kindler, S. H., and Rosenberg, E. (1977) Myxospore coat synthesis in *Myxococcus xanthus*: in vivo incorporation of acetate and glycine. *J Bacteriol* **131**, 751-758
29. Behmlander, R. M., and Dworkin, M. (1994) Biochemical and structural analyses of the extracellular matrix fibrils of *Myxococcus xanthus*. *J Bacteriol* **176**, 6295-6303
30. Maclean, L., Perry, M. B., Nossova, L., Kaplan, H., and Vinogradov, E. (2007) The structure of the carbohydrate backbone of the LPS from *Myxococcus xanthus* strain DK1622. *Carbohydr Res* **342**, 2474-2480
31. Guo, D., Wu, Y., and Kaplan, H. B. (2000) Identification and characterization of genes required for early *Myxococcus xanthus* developmental gene expression. *J Bacteriol* **182**, 4564-4571
32. Lu, A., Cho, K., Black, W. P., Duan, X. Y., Lux, R., Yang, Z., Kaplan, H. B., Zusman, D. R., and Shi, W. (2005) Exopolysaccharide biosynthesis genes required for social motility in *Myxococcus xanthus*. *Mol Microbiol* **55**, 206-220
33. Chao, L., and Bowen, C. C. (1971) Purification and properties of glycogen isolated from a blue-green alga, *Nostoc muscorum*. *J Bacteriol* **105**, 331-338
34. Nariya, H., and Inouye, S. (2003) An effective sporulation of *Myxococcus xanthus* requires glycogen consumption via Pkn4-activated 6-phosphofructokinase. *Mol Microbiol* **49**, 517-528
35. Whitfield, C. (2006) Biosynthesis and assembly of capsular polysaccharides in *Escherichia coli*. *Annu Rev Biochem* **75**, 39-68
36. Ueki, T., and Inouye, S. (2005) Identification of a gene involved in polysaccharide export as a transcription target of FruA, an essential factor for *Myxococcus xanthus* development. *J Biol Chem* **280**, 32279-32284
37. Schnaitman, C. A. (1971) Solubilization of the cytoplasmic membrane of *Escherichia coli* by Triton X-100. *J Bacteriol* **108**, 545-552
38. Lobedanz, S., and Sogaard-Andersen, L. (2003) Identification of the C-signal, a contact-dependent morphogen coordinating multiple developmental responses in *Myxococcus xanthus*. *Genes Dev* **17**, 2151-2161
39. Bulyha, I., Schmidt, C., Lenz, P., Jakovljevic, V., Hone, A., Maier, B., Hoppert, M., and Sogaard-Andersen, L. (2009) Regulation of the type IV pili molecular machine by dynamic localization of two motor proteins. *Mol Microbiol* **74**, 691-706
40. Orndorff, P. E., and Dworkin, M. (1980) Separation and properties of the cytoplasmic and outer membranes of vegetative cells of *Myxococcus xanthus*. *J Bacteriol* **141**, 914-927
41. Simunovic, V., Gherardini, F. C., and Shimkets, L. J. (2003) Membrane localization of motility, signaling, and polyketide synthetase proteins in *Myxococcus xanthus*. *J Bacteriol* **185**, 5066-5075
42. Higgs, P. I., Letain, T. E., Merriam, K. K., Burke, N. S., Park, H., Kang, C., and Postle, K. (2002) TonB interacts with nonreceptor proteins in the outer membrane of *Escherichia coli*. *J Bacteriol* **184**, 1640-1648
43. Takeda, M., Kondo, K., Yamada, M., Koizumi, J., Mashima, T., Matsugami, A., and Katahira, M. (2010) Solubilization and structural determination of a glycoconjugate which is assembled into the sheath of *Leptothrix cholodnii*. *Int J Biol Macromol* **46**, 206-211

44. Nishiyama, Y., Langan, P., and Chanzy, H. (2002) Crystal structure and hydrogen-bonding system in cellulose I β from synchrotron X-ray and neutron fiber diffraction. *J Am Chem Soc* **124**, 9074-9082
45. Kameda, T., Miyazawa, M., Ono, H., and Yoshida, M. (2005) Hydrogen bonding structure and stability of alpha-chitin studied by ¹³C solid-state NMR. *Macromol Biosci* **5**, 103-106
46. Holtje, J. V. (1998) Growth of the stress-bearing and shape-maintaining murein sacculus of *Escherichia coli*. *Microbiol Mol Biol Rev* **62**, 181-203
47. Steber, J., and Schleifer, K. H. (1975) *Halococcus morrhuae*: a sulfated heteropolysaccharide as the structural component of the bacterial cell wall. *Arch Microbiol* **105**, 173-177
48. Niemetz, R., Karcher, U., Kandler, O., Tindall, B. J., and Konig, H. (1997) The cell wall polymer of the extremely halophilic archaeon *Natronococcus occultus*. *Eur J Biochem* **249**, 905-911
49. Mio, T., Yamada-Okabe, T., Arisawa, M., and Yamada-Okabe, H. (1999) *Saccharomyces cerevisiae* GNA1, an essential gene encoding a novel acetyltransferase involved in UDP-N-acetylglucosamine synthesis. *J Biol Chem* **274**, 424-429
50. Kimura, Y., Kato, T., and Mori, Y. (2012) Function analysis of a bacterial tyrosine kinase, BtkB, in *Myxococcus xanthus*. *FEMS Microbiol Lett*
51. Woodward, R., Yi, W., Li, L., Zhao, G., Eguchi, H., Sridhar, P. R., Guo, H., Song, J. K., Motari, E., Cai, L., Kelleher, P., Liu, X., Han, W., Zhang, W., Ding, Y., Li, M., and Wang, P. G. (2010) In vitro bacterial polysaccharide biosynthesis: defining the functions of Wzy and Wzz. *Nat Chem Biol* **6**, 418-423
52. Morona, J. K., Paton, J. C., Miller, D. C., and Morona, R. (2000) Tyrosine phosphorylation of CpsD negatively regulates capsular polysaccharide biosynthesis in *Streptococcus pneumoniae*. *Mol Microbiol* **35**, 1431-1442
53. Niemeyer, D., and Becker, A. (2001) The molecular weight distribution of succinoglycan produced by *Sinorhizobium meliloti* is influenced by specific tyrosine phosphorylation and ATPase activity of the cytoplasmic domain of the ExoP protein. *J Bacteriol* **183**, 5163-5170
54. Licking, E., Gorski, L., and Kaiser, D. (2000) A common step for changing cell shape in fruiting body and starvation-independent sporulation of *Myxococcus xanthus*. *J Bacteriol* **182**, 3553-3558
55. Kimura, Y., Yamashita, S., Mori, Y., Kitajima, Y., and Takegawa, K. (2011) A *Myxococcus xanthus* bacterial tyrosine kinase, BtkA, is required for the formation of mature spores. *J Bacteriol* **193**, 5853-5857
56. Bushell, S. R., Mainprize, I. L., Wear, M. A., Lou, H., Whitfield, C., and Naismith, J. H. (2013) Wzi is an outer membrane lectin that underpins group 1 capsule assembly in *Escherichia coli*. *Structure* **21**, 844-853
57. Gorke, B., Foulquier, E., and Galinier, A. (2005) YvcK of *Bacillus subtilis* is required for a normal cell shape and for growth on Krebs cycle intermediates and substrates of the pentose phosphate pathway. *Microbiology* **151**, 3777-3791
58. Cserzo, M., Wallin, E., Simon, I., von Heijne, G., and Elofsson, A. (1997) Prediction of transmembrane alpha-helices in prokaryotic membrane proteins: the dense alignment surface method. *Protein Eng* **10**, 673-676
59. Bhat, S., Zhu, X., Patel, R. P., Orlando, R., and Shimkets, L. J. (2011) Identification and localization of *Myxococcus xanthus* porins and lipoproteins. *PLoS ONE* **6**, e27475
60. Garner, E. C., Bernard, R., Wang, W., Zhuang, X., Rudner, D. Z., and Mitchison, T. (2011) Coupled, circumferential motions of the cell wall synthesis machinery and MreB filaments in *B. subtilis*. *Science* **333**, 222-225
61. Dominguez-Escobar, J., Chastanet, A., Crevenna, A. H., Fromion, V., Wedlich-Soldner, R., and Carballido-Lopez, R. (2011) Processive movement of MreB-associated cell wall biosynthetic complexes in bacteria. *Science* **333**, 225-228
62. Pallen, M., Chaudhuri, R., and Khan, A. (2002) Bacterial FHA domains: neglected players in the phospho-threonine signalling game? *Trends Microbiol* **10**, 556-563
63. Kaiser, D. (1979) Social gliding is correlated with the presence of pili in *Myxococcus xanthus*. *Proc Natl Acad Sci U S A* **76**, 5952-5956

64. Bowden, M. G., and Kaplan, H. B. (1998) The *Myxococcus xanthus* lipopolysaccharide O-antigen is required for social motility and multicellular development. *Mol Microbiol* **30**, 275-284
65. Julien, B., Kaiser, A. D., and Garza, A. (2000) Spatial control of cell differentiation in *Myxococcus xanthus*. *Proc Natl Acad Sci U S A* **97**, 9098-9103
66. Wu, S. S., and Kaiser, D. (1996) Markerless deletions of *pil* genes in *Myxococcus xanthus* generated by counterselection with the *Bacillus subtilis* *sacB* gene. *J Bacteriol* **178**, 5817-5821
67. Marchler-Bauer, A., Anderson, J. B., DeWeese-Scott, C., Fedorova, N. D., Geer, L. Y., He, S., Hurwitz, D. I., Jackson, J. D., Jacobs, A. R., Lanczycki, C. J., Liebert, C. A., Liu, C., Madej, T., Marchler, G. H., Mazumder, R., Nikolskaya, A. N., Panchenko, A. R., Rao, B. S., Shoemaker, B. A., Simonyan, V., Song, J. S., Thiessen, P. A., Vasudevan, S., Wang, Y., Yamashita, R. A., Yin, J. J., and Bryant, S. H. (2003) CDD: a curated Entrez database of conserved domain alignments. *Nucleic Acids Res* **31**, 383-387
68. Yu, C. S., Chen, Y. C., Lu, C. H., and Hwang, J. K. (2006) Prediction of protein subcellular localization. *Proteins* **64**, 643-651

Acknowledgements - This research was supported by the Deutsche Forschungsgemeinschaft (grant HI1593/2-1 to PH), Wayne State University (PH), a fellowship from the International Max Planck Research School (CH), and the National Institutes of Health GM85024 (EH). The authors gratefully acknowledge Dr. Annika Ries, Dr. Oliver Ries, and Dr. Chris van der Does for invaluable discussions, Dr. Kathleen Postle for sharing detailed density gradient fractionation protocols, and past and present members of the Higgs and Hoiczky labs for helpful discussion and proofreading of the manuscript. We gratefully acknowledge Petra Mann for excellent technical assistance.

FOOTNOTES

¹The abbreviations used are: EPS, exopolysaccharide; O-Ag, O-Antigen; Glc, glucose; CCRC, Complex Carbohydrate Research Center; TMS, trimethylsilyl; DIC, differential interference contrast; CM, cytoplasmic membrane; OM, outer membrane; IPTG, Isopropyl β -D-1-thiogalactopyranoside; GlcNAc, N-acetyl-glucosamine; und-PP, undecaprenol di-phosphate; pmf, proton motive force.

FIGURE LEGENDS

FIGURE 1. Negative stain electron microscopy of material isolated during spore coat purification. Wild type (wt; strain DK1622), Δ *exoC* (PH1261), Δ *exoC wzm epsV* (PH1296), and Δ *nfsA-H* (Δ *nfs*; PH1200) cells were induced to sporulate for four hours by addition of glycerol and subject to a spore coat isolation protocol. Representative pictures at lower (top panels) and higher (bottom panels) magnifications are shown. Bar corresponds to 1 μ m for wt, Δ *exoC*, and Δ *nfsA-H* panels, and 500 nm for Δ *exoC wzm epsV* panels. Arrows point to particles in the wild type similar to those isolated from the Δ *exoC wzm epsV* mutant.

FIGURE 2. The amino acid and amino sugar composition of the material recovered in a spore coat isolation protocol. Wild type (wt; DK1622), Δ *exoC* (PH1261), *wzm epsV* (PH1285), and Δ *nfsA-H* (Δ *nfs*; PH1200) cells were induced to sporulate for four hours by addition of glycerol. Material was isolated, acid-hydrolysed and a sample volume corresponding to 0.2 mg protein per lane was loaded on a cellulose TLC plate and stained with ninhydrin. Marker: 2 μ l of 10 mM each glutamate, glycine, alanine and galactosamine in water. Spots 1, 2, and 3, which were further analyzed by mass spectrometry, are indicated to the right.

FIGURE 3. Sporulation phenotype of mutants bearing individual *exo* gene deletions. Vegetative cells from wt (wt; DK1622), Δ *exoC* (PH1261), Δ *nfsA-H* (Δ *nfs*; PH1200), Δ *exoB* (PH1303), Δ *exoD* (PH1304), Δ *exoE* (PH1265), Δ *exoF* (PH1507), Δ *exoG* (PH1508), Δ *exoH* (PH1264), Δ *exoI* (PH1511), and Δ MXAN_1305 (PH1509) were induced for sporulation with glycerol and examined by DIC and phase microscopy at the indicated hours. Bar, 2 μ m. The sporulation efficiency after 24 hours of induction is displayed in white text (24 hr. phase pictures) as the average and associated standard deviation of three biological replicates.

FIGURE 4. The amino acid and amino sugar composition of spore coat material recovered from individual *exo* mutants. Wild type (wt; DK1622), Δ *exoB* (PH1303), Δ *exoD* (PH1304), Δ *exoE* (PH1265), Δ *exoF* (PH1507), Δ *exoG* (PH1508), Δ *exoH* (PH1264), Δ *exoI* (PH1511), Δ *exoC* (PH1261) and Δ *nfsA-H* (Δ *nfs*; PH1200) cells induced to sporulate for four hours by addition of glycerol. Material was isolated, acid-hydrolysed and a sample volume corresponding to 0.2 mg protein per lane was loaded on a cellulose TLC plate and stained with ninhydrin. Marker: 2 μ l of 10 mM glutamate, glycine, alanine and galactosamine in water.

FIGURE 5. Membrane localization of Nfs proteins produced in *E. coli*. Sucrose density gradient fractionations of *E. coli* BL21DE3 cells producing NfsA and B (**A**), NfsC (**B**), or NfsD, E, and G (**C**) from plasmids pCH20, pCH57, and pCH21, respectively. A-C: top graph: NADH oxidase activity as a marker for cytoplasmic membrane fractions measured in the indicated fractions. Middle panel: Total proteins from each indicated fraction resolved by denaturing polyacrylamide gel electrophoresis followed by Coomassie stain. OmpC/F are indicated as a marker for outer membrane fractions. Asterisk represents NfsC in **B**. Bottom panel(s): Immunoblot analysis of the indicated fractions probed with anti-NfsA and anti-NfsB antisera (**A**), anti-NfsC antisera (**B**) and anti-NfsD, anti-NfsE, or anti-NfsG sera (**C**) as indicated in the fractions indicated. Proteins from uninduced (U) and induced (I) whole cells and from lysates of induced cells expressing the respective plasmid (L) or empty vector (V) are shown. NfsG is detected as full length (top arrow), and degradation product (bottom arrow).

FIGURE 6. Working model of spore coat production and assembly in *M. xanthus*. GalNAc and Glu (11-17:1) polymers are synthesized and secreted to the cell surface by the Exo proteins (Red text) and assembled into a stress-bearing structure by the Nfs proteins (Blue text). The Exo proteins resemble a Wzy-dependent capsule secretion machinery; respective homologs are identified in black text. Und-PP linked carbohydrate repeat units are generated on the inner surface of the cytoplasmic membrane (CM) by ExoE and the ExoF-I processing enzymes (step1), translocated to the outer surface of the CM by an unidentified flippase (Wzx) (step 2), and polymerized by Wzy (likely MXAN_3026) (5) (step 3). Polymers are secreted to the cell surface by the terminal export complex consisting of ExoC/D and ExoA (step 4). The Nfs proteins, are located in either the outer membrane (OM) or CM as indicated. NfsG interacts with a TolQRS energy harvesting complex (13) (not shown). The Nfs proteins are necessary for assembly of the capsule-like carbohydrates into a rigid sacculus in a process that involves an apparent increase in the proportion of terminal Glc and GalNAc residues. This process may involve cleavage of polysaccharides chains on the cell surface (step 5a) or influence of polysaccharide extrusion via interaction with ExoC/D (step 5b). See text for details. Inset: A possible arrangement of the spore coat in which glycine peptides (Gly_n) replaces the acetyl group in certain GalNAc residues to bridge to the C1 carbon of an adjacent glycan. See text for details.

TABLES

Table 1. Strains and plasmids used in this study.

Strain or plasmid	Genotype	Reference or source
<i>Myxococcus xanthus</i>		
DK1622	Wild type	(63)
PH1261	DK1622 Δ <i>exoC</i>	(5)
PH1200	DK1622 Δ <i>nfsA-H</i>	(9)
PH1303	DK1622 Δ <i>exoB</i>	This study
PH1304	DK1622 Δ <i>exoD</i>	This study
PH1265	DK1622 Δ <i>exoE</i>	This study
PH1507	DK1622 Δ <i>exoF</i>	This study
PH1508	DK1622 Δ <i>exoG</i>	This study
PH1264	DK1622 Δ <i>exoH</i>	This study
PH1511	DK1622 Δ <i>exoI</i>	This study
PH1509	DK1622 Δ MXAN_1035	This study
PH1270	DK1622 <i>wzm</i> :: Ω Kan ^R	This study
PH1285	DK1622 <i>wzm</i> :: Ω Kan ^R <i>epsV</i> ::pCH19	This study
PH1296	DK1622 Δ <i>exoC</i> <i>wzm</i> :: Ω Kan ^R <i>epsV</i> ::pCH19	This study
HK1321	DK1622 <i>wzm</i> :: Ω Kan ^R	(18,64)
<i>Escherichia coli</i>		
TOP10	Host for cloning [F ⁻ <i>mcrA</i> Δ (<i>mrr</i> - <i>hsdRMS-mcrBC</i>) Φ 80 <i>lacZ</i> Δ M15 Δ <i>lacX74</i> <i>deoR</i> <i>recA1</i> <i>arsD139</i> Δ (<i>ara-leu</i>)7697 <i>galU</i> <i>halK</i> <i>rpsL</i> (Str ^r) <i>endA1</i> <i>nupG</i>]	Invitrogen
BL21(DE3)	Host for overexpression (<i>fhuA2</i> [<i>lon</i>] <i>ompT</i> <i>gal</i> (λ DE3) [<i>dcm</i>] Δ <i>hsdS</i>)	Novagen
Plasmids		
pBJ114	Backbone for in-frame deletions; <i>galK</i> , Kan ^R	(65)
pUC19	cloning vector, Amp ^R	Thermo Scientific
pSW30	Source of Tc ^R cassette	(66)
pCDF-Duet	Pr _{T7} , Spc ^R	Novagen
pCOLA-Duet	Pr _{T7} , Kan ^R	Novagen
pCH14-2	pBJ114 Δ <i>exoE</i> (aa 5-451)	This study
pCH15-1	pBJ114 Δ <i>exoH</i> (aa 11-374)	This study
pCH48	pBJ114 Δ <i>exoG</i> (codons 16-337)	This study
pCH49	pBJ114 Δ <i>exoF</i> (codons 26-351)	This study
pCH50	pBJ114 Δ <i>exoI</i> (codons 8-381)	This study
pCH51	pBJ114 Δ <i>exoB</i> (codons 16-388)	This study
pCH63	pBJ114 Δ <i>exoD</i> (codons 7-215)	This study
pCH62	pBJ114 Δ MXAN_1035 (codons 14-473)	This study
pCH19	Internal fragments of <i>epsV</i> (codons	This study

	323-500) and Tc ^R in pUC19	
pCH20	The <i>nfsA-C</i> coding region in pCDF-Duet	This study
pCH21	The <i>nfsD-H</i> coding region in pCOLA-Duet	This study
pCH57	The coding region of <i>nfsC</i> in pCDF-Duet	This study

Table 2. Glycosyl composition in spore coat material isolated from strains bearing the indicated genotypes.

genotype (strain)	μg material per 10^8 cells				
	wt (DK1622)	<i>wzm epsV</i> (PH1285)	ΔexoC (PH1261)	ΔexoC <i>wzm epsV</i> (PH1296)	Δnfs (PH1200)
dry weight	148	89	46	8	180
estimated % carbohydrate	92	81	64	30	85
(N-acetyl) galactosamine	94	61	ND	ND	113
glucose	24	7	20	3	28
(N-acetyl) glucosamine	8	5	3	ND	5
xylose	5	ND	3	ND	3
rhamnose	5	ND	3	ND	4
mannose	1	ND	<1	ND	<1
galactose	<1	ND	<1	<<1	<1

ND: none detected

Table 3. Predicted characteristics of the Exo proteins

Gene	Locus I	Predicted function (Predicted domain accession; expect value) ¹	Localization ²
<i>exoA</i>	MXAN_3225	polysaccharide biosynthesis/export (COG1596; 1.4e ⁻³³)	OM (11)
<i>exoB</i>	MXAN_3226	hypothetical protein	OM
<i>exoC</i>	MXAN_3227	chain length determinant family (COG3206; 1.1e ⁻²⁰)	CM
<i>exoD</i>	MXAN_3228	tyrosine kinase (TIGR03018; 6.5e ⁻³⁷)	S
<i>exoE</i>	MXAN_3229	polyprenyl glycosylphosphotransferase (TIGR03025; 7.1e ⁻¹¹⁴)	CM
<i>exoF</i>	MXAN_3230	YvcK-like (cd07187; 3.4e ⁻¹²⁶)	S
<i>exoG</i>	MXAN_3231	N-Acetyltransferase (GNAT) (pfam13480; 2.3e ⁻³²)	S
<i>exoH</i>	MXAN_3232	3-amino-5-hydroxybenzoic acid synthase family (cd00616; 6.6e ⁻²⁹)	S
<i>exoI</i>	MXAN_3233	N-Acetyltransferase (GNAT) (pfam13480; 6.9e ⁻³³)	S

¹The putative function/domains were predicted by NCBI conserved domain search (67).

²Localization was predicted by CELLO (68), unless otherwise indicated. OM, outer membrane; S, soluble (*i.e.* cytoplasmic or periplasmic); CM, cytoplasmic membrane.

Table 4. Glucose (Glc) and N-Acetylgalactosamine [GalNAc] linkages identified in spore coat material isolated from wild type (wt) $\Delta nfsA-H$ (Δnfs) strains.

residue	Genotype (strain)	
	wt (DK1622)	Δnfs (PH1200)
GalNAc	100	100
t-GalNAc	41 ± 0	3 ± 1
4-GalNAc	44 ± 3	62 ± 8
3-GalNAc	15 ± 2	32 ± 5
3,4-GalNAc	ND	1 ± 1
4,6-GalNAc	ND	1 ± 2
Glc	100	100
t-Glc	26 ± 2	12 ± 3
6-Glc	6 ± 3	2 ± 0
4-Glc	64 ± 3	83 ± 6
3,4-Glc	1 ± 2	1 ± 1
2,4-Glc	1 ± 1	1 ± 1
4,6-Glc	2 ± 0	1 ± 1
2,3,4,6-Glc	ND	1 ± 1

Average and standard deviation of two independent analyses from independent biological replicates.

Fig. 1

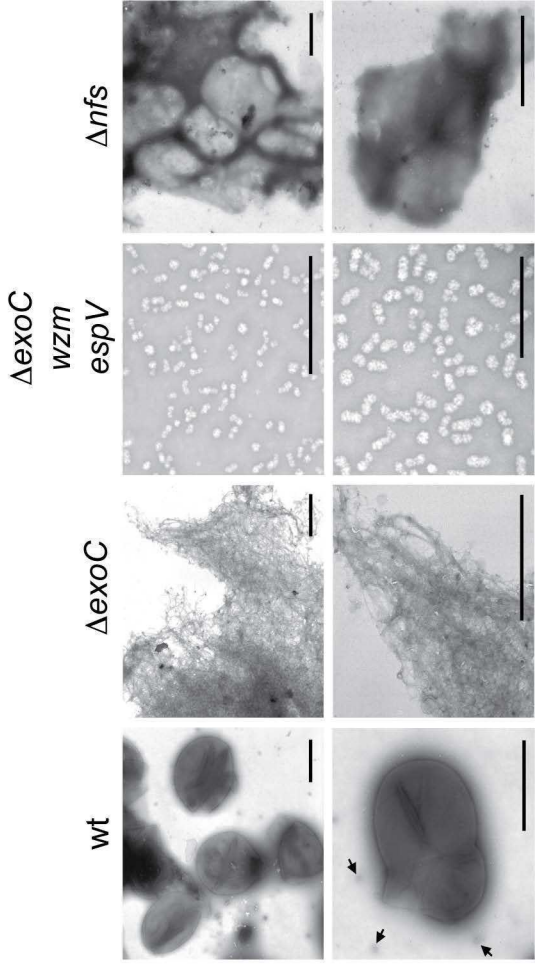


Fig. 2

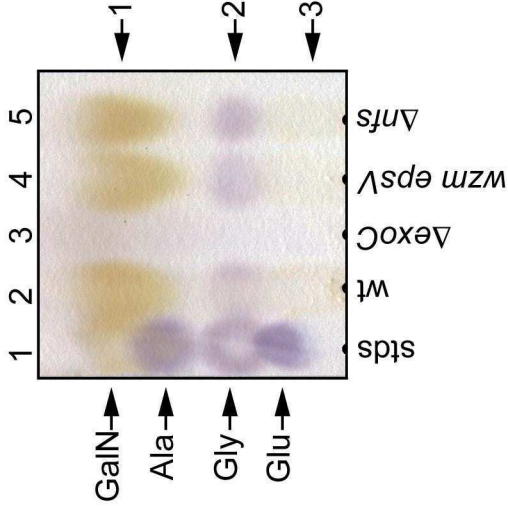


Fig. 3

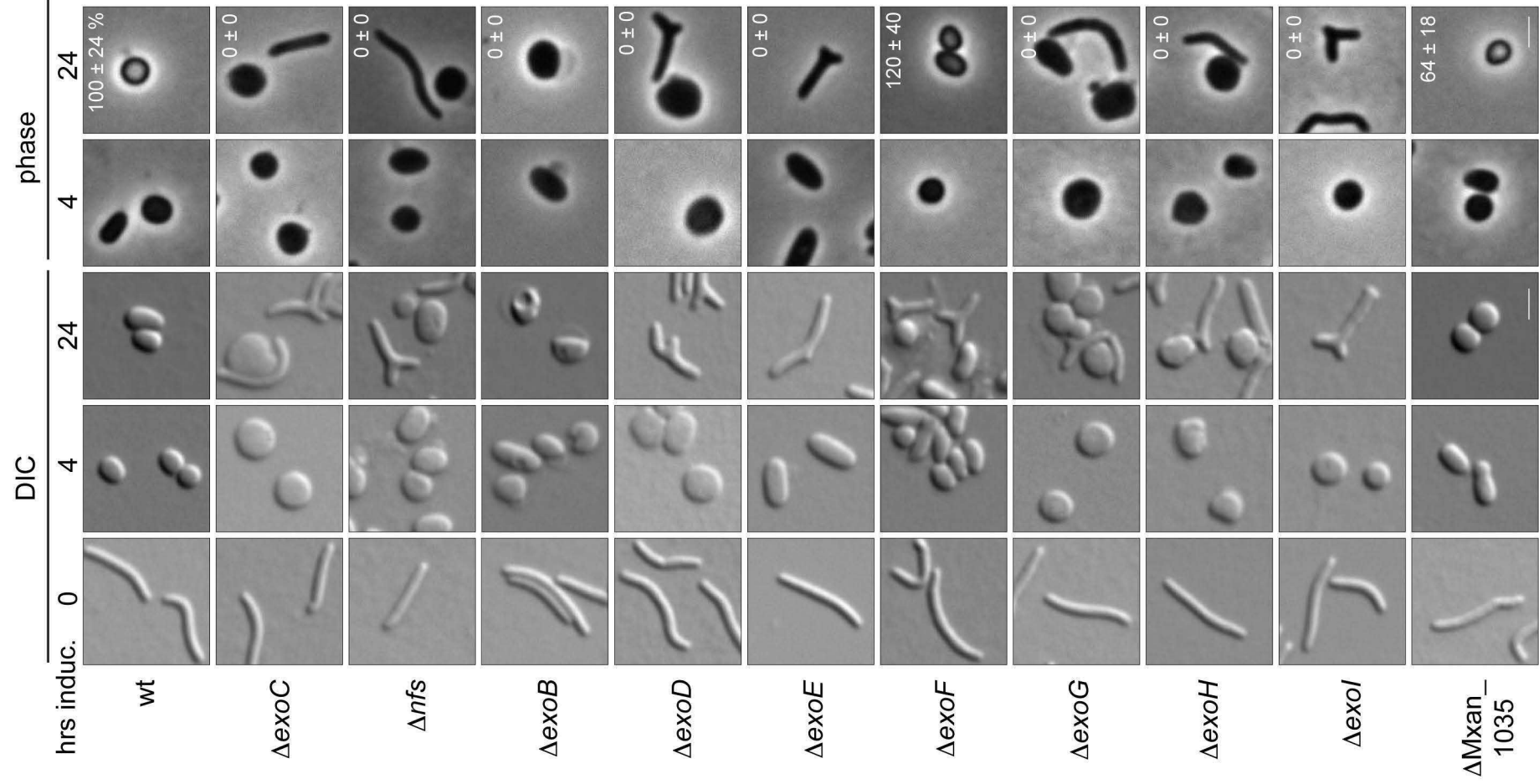


Fig. 4

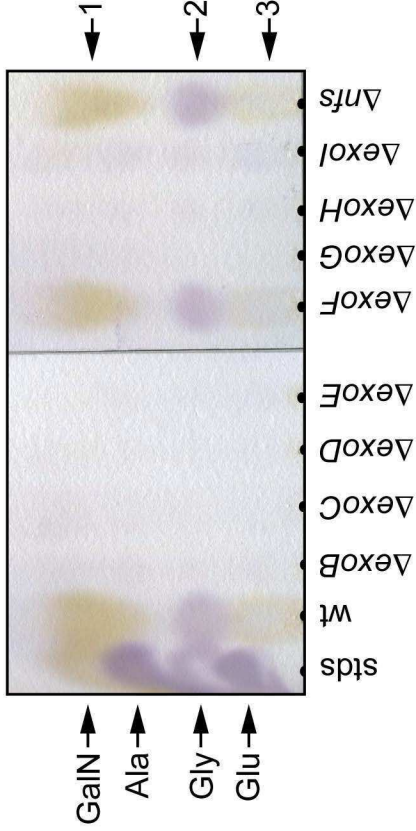


Fig. 6

